Journal of Himalayan Earth Sciences Volume 57, No. 1, 2024 pp. 01-22

Integrated Petrographical, Mineralogical, and Geochemical Investigation to Evaluate Diagenesis of Sandstone: A Case Study of the Oligocene Nari Formation from Southern Kirthar Range, Pakistan

Surriya Bibi Ahmedani[1,2*], Muhammad Hassan Agheem[1], Asghar A. A. D. Hakro[1], Aijaz Ali Halepoto[1], Rafique Ahmed Lashari[1], and Ghulam Mustafa Thebo[1]

[1]*Centre for Pure and Applied Geology, Faculty of Natural Sciences, University of Sindh, Jamshoro, Pakistan*

[2]*Government Zubeda Girls College, Hyderabad, College Education Department, Government of Sindh, Pakistan*

**Corresponding author: suriyabibi128@yahoo.com*

Submitted date: 06/09/2023 Accepted date: 26/02/2024 Published online: 31/03/2024

Abstract

In this work, the sandstone facies of the Nari Formation from the Nari River Section in Southern Kirthar Range, Pakistan are studied to decipher their diagenetic processes, stages, and associated tectonic events using petrographic, mineralogical, and geochemical analysis. The field study encompasses outcrop observations, section measurement and sampling. Laboratory work includes thin-section preparation and analysis of the samples under a petrographic microscope, X-Ray Diffraction, Scanning Electron Microscopy, and Energy Dispersive X-Ray Spectroscopy. During this study, different diagenetic processes, such as cementation, compaction, quartz dissolution, quartz overgrowth, and grain deformation porosity are identified. Results indicate that iron oxide is the most abundant cementing material in samples followed by calcite and dolomite. The cement has completely destroyed the primary porosity. The sandstone of the Nari Formation indicates poor to well compaction as exhibited by grain contacts. Identified diagenetic processes are classified into three diagenetic stages, which are eogenesis, mesogenesis and telogenesis. Eogenesis is contemporary to the deposition of Nari Formation. Nari Formation experienced mesogenesis during the Pliocene. Deformation and uplifting of the north-western margin of the Indian Plate during the Pliocene-Pleistocene brought the Nari Formation into the regime of telogenesis. This study suggests that the diagenesis of the Nari Formation is controlled by the Oligocene-Pleistocene tectonic evolution of the study area. This integrated and comprehensive investigation not only provides important constraints on the diagenetic history of the Nari Formation but also accentuates the crucial role played by the Oligocene-Pleistocene tectonic evolution to control the diagenesis of the Nari Formation in the study area. The present work will serve as a demonstration of the critical interaction between diagenetic processes and tectonic events in the evolution of sedimentary formations thereby offering valuable insights for both academic understanding and geological resource exploration.

Keywords: Petrography; Geochemistry; Diagenesis; Sandstone; Nari Formation; Kirthar Range of Pakistan.

1. Introduction

The economic significance of sedimentary rocks like shale as a source rock and sandstone as a reservoir rock for hydrocarbons depends upon diagenesis (Worden and Burley, 2003). Nowadays, special attention is being paid to the exploration of new geological reservoirs for not only hydrocarbons but also for CO_2 sequestration and energy storage (Bickle, 2009; Kelemen et al., 2019; Zhang et al., 2023; Chen et al., 2023; Bashir et al., 2024). Reservoir quality is an important controlling factor in prospect evaluation. Hence, it is imperative to gain a detailed perceptive of those factors that control the reservoir quality of a rock to aid with the evaluation of the economic feasibility of petroleum discoveries (Selley, 1998; Ashraf et al., 2020; Anees et al., 2022; Rashid et al., 2022; Hansen et al., 2023). The reservoir quality in clastic rocks is determined by several relevant factors such as mineralogy, pore water chemistry, diagenesis, temperature, fluid flow, environment of deposition, tectonic setup, burial depth, uplifting, and geothermal gradient (Bjorlykke, 1988; Zou et al., 2012). Reconstruction of the diagenetic history of rock plays a vital role in understanding reservoir porosity and permeability to envisage the reservoir characteristics of clastic sedimentary rocks (Salem et al., 2005; Honarmand and Amini, 2012). Over the last twenty years, several workers such as Bloch et al. (2002); Worden and Burley (2003); Mackenzie (2005); Reed et al. (2005); Gier et al. (2008); Ajdukiewicz and Lander (2010); and Baiyegunhi et al. (2017) have acknowledged the relationship between diagenesis and reservoir quality of the sandstone. Petrography has a key significance for the recognition of the different diagenetic processes and their effects on the porosity and permeability of sandstones and other clastic rocks (Ajdukiewicz and Lander, 2010; Umar et al., 2011; Dars et al., 2020; Dar et al., 2022; Ullah et al., 2022).

Nari Formation was deposited during the Oligocene, which was the time of the India-Eurasia collision and commencement of Himalayan Orogeny (Powell, 1979; Bannert et al., 1992; Ding et al., 2016; Jadoon et al., 2020; Ghani et al., 2023; Jadoon et al., 2024). The development of Kirthar and Suleiman fold belts also started during the Oligocene. Kirthar Fold Belt forms the southernmost part of the regional Himalayan-Tibetan Orogenic Belt and is located in the western part of the Southern Indus Basin (Bannert et al., 1992; Smewing et al., 2002; Hinsch et al., 2019; Halepoto et al., 2023) (Figure 1a). Kirthar Fold Belt is Contemporaneous to the Zagros Fold Belt of Iran and the Carpathian Fold Belt of the Alps. Kirthar Range is part of the Kirthar Fold Belt (Kazmi and Jan, 1997). Nari Formation is widely distributed in the Kirthar Fold Belt and Southern Suleiman Fold Belt. However, it is thicker in the Kirthar Fold Belt than Suleiman Fold Belt (Cheema et al., 2009). The Nari Nai (locally known as Nali Nai) section is located in southern part of the Kirthar Range (Figure 1a). Nari Formation consists of sandstone interbedded with shale and minor claystone in the studied section. The Nari Formation is previously studied in terms of fossils (Duncan and Sladen, 1884; Vredenburg, 1925), textural evaluation (Khokhar et al., 2016), reservoir potential (Mahmud and Sheikh, 2009), composition and provenance (Ahmed et al., 2020), depositional environment (Hakro et al., 2021; Samtio et al., 2021), the influence of diagenetic features on petrophysical properties (Shar et al., 2021a), petrography and geochemistry (Shar et al., 2021b), petrography (Paryal et al., 2020) and major element composition (Hakro et al., 2022). All the previous work on the Nari Formation is carried out in the Karachi arc (Figure 1a) of Pakistan. There is a significant difference between the depositional and tectonic architecture of Nari Formation between the Kirthar Range and the Karachi arc of the Southern Indus Basin. Distinct diagenetic features and stages of Nari Formation sandstone and their relationship with the late Tertiary and Quaternary tectonic deformation of north-western edge of the Indian Plate is poorly understood. In present work, we carried out detailed diagenetic study of sandstone of Nari Formation to identify different diagenetic stages. Based on the results obtained from the data, we discussed different diagenetic processes, tectonic importance of the diagenesis and reservoir quality of the Nari Formation in the Kirthar Range, Pakistan.

1.1. Stratigraphy of the studied section

In the study area, the stratigraphic section as per chronological order is Kirthar Formation of Late Eocene age, Nari Formation of Oligocene age, Gaj Formation of Miocene, Manchar Formation of Mio-Pliocene and Dada Conglomerate of Pleistocene (Hunting Survey Corporation, 1960; Cheema et al., 2009) (Figure 1b). Nari Formation overlies the Kirthar Formation whereas its upper contact with the Gaj Formation is unconformable and is marked by alternating beds of laterite and sandstone (Table 1). Khan (1968) proposed Rupelian to the early Aquitanian age to the Nari Formation.

Nari Formation is divided into lower and upper parts based on bed thickness, interbedded lithology, lithification and oxidation, in the studied section. The lower part ranges from sample number NR-1 to NR-16 in the columnar section (Figure 2). The sandstone of the lower part is thin to thick-bedded, well lithified, interbedded with shale, oxidized and calcareous. The upper part of the formation ranges from sample number NR-17 to NR-33 in the columnar section (Figure 2). The sandstone of the upper part is thick-bedded to massive, jointed, poorly compacted to friable, and occasionally intercalated with gypsiferous claystone (Figure 3a). Sandstone exhibits primary sedimentary structures such as ripple marks (Figure 3b) and cross-stratification (Figure 3c).

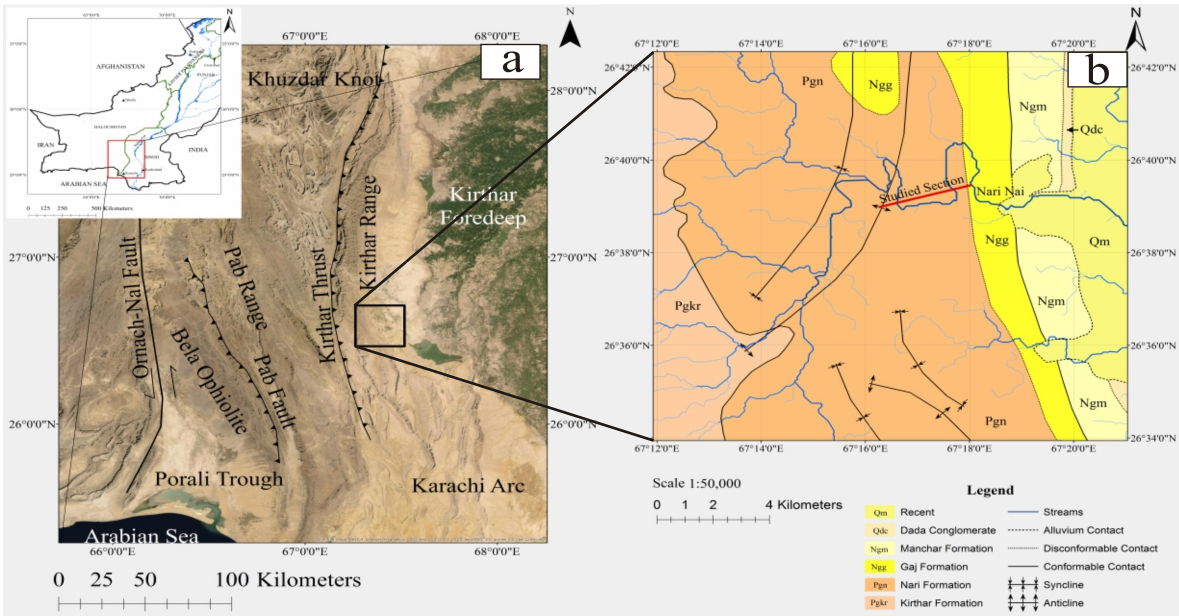

Fig. 1. (a) Shows locations of the study area (Rectangle) and (b) Geological map showing different stratigraphic sections (bold red line represents studied section) of the Southern Kirthar Range, Pakistan (modified after Hunting Survey Corporation (1960) and Ghani et al. (2023)

Table 1: General stratigraphic succession of the study area (After Hunting Survey Corporation, 1960; Shah, 1977).

Era	Period	Epoch	Formation	Lithology
Cenozoic	Quaternary	Recent	Alluvium	Sand, Silt, and Clay
		Pleistocene	Dada Conglomerate	Conglomerate
	Tertiary	Pliocene	Manchar Formation	Sandstone
		Miocene	Gaj Formation	Sandstone and Shale
		Oligocene	Nari Formation	Limestone, Sandstone and Shale
		Eocene	Kirthar Formation	Limestone

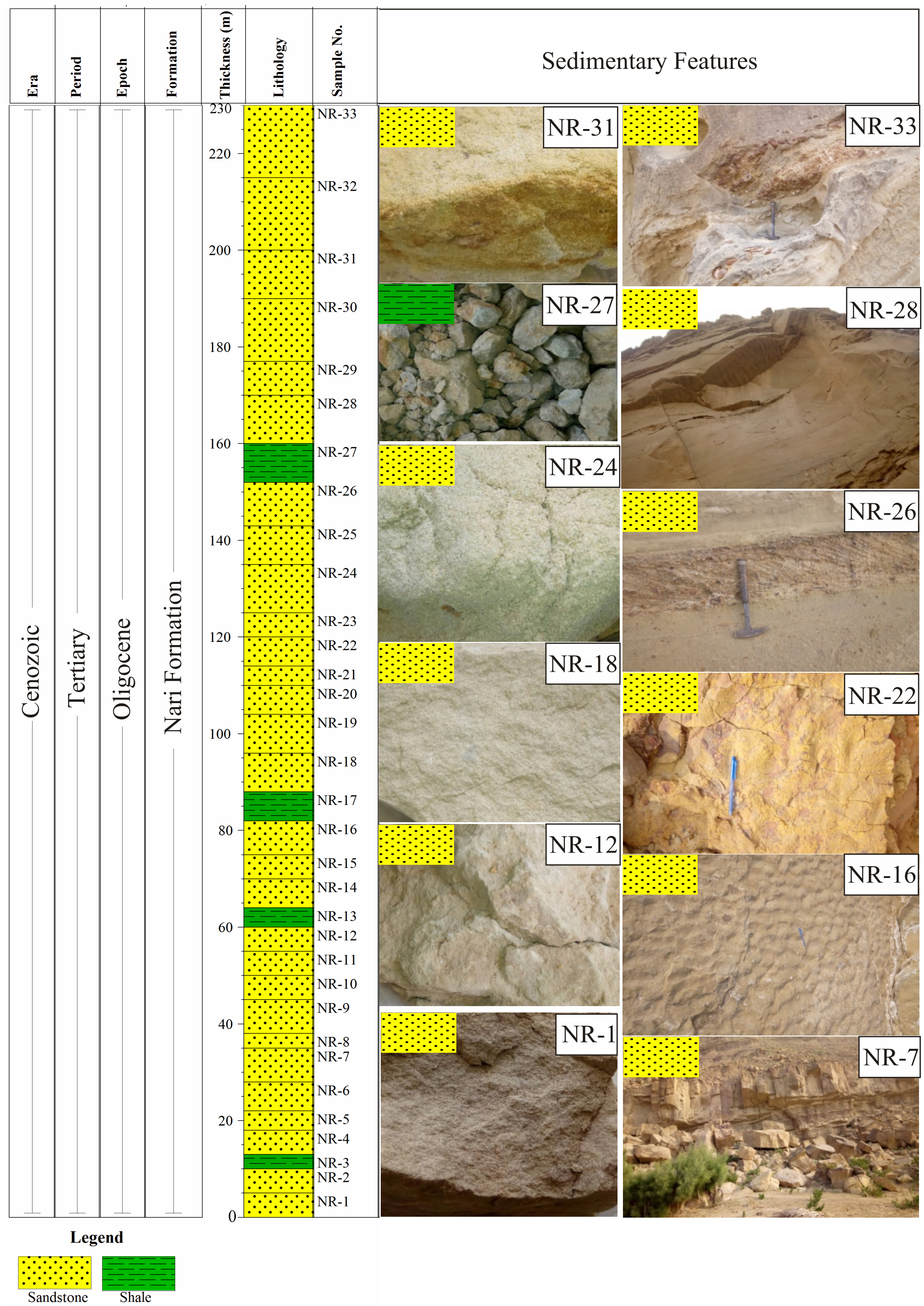

Fig. 2. Columnar Section of Nari Formation in Nari Nai section, Southern Kirthar Range, Pakistan.

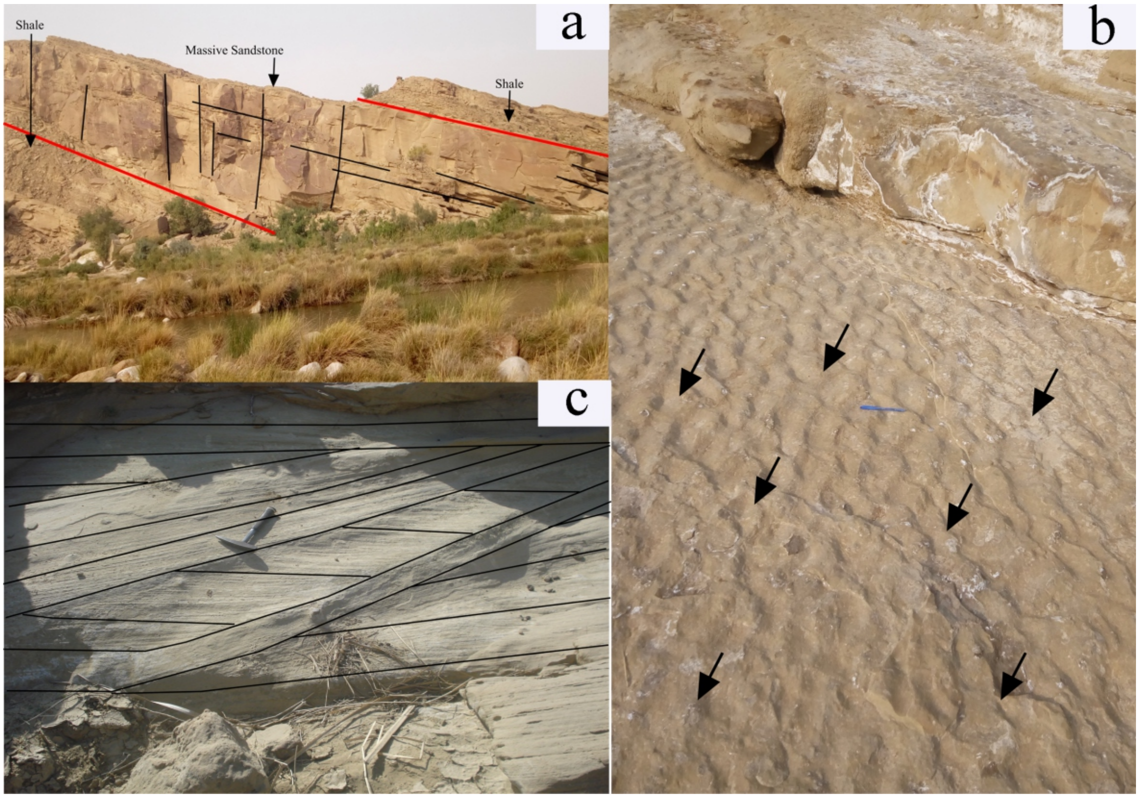

Fig. 3. Field Image showing (a) jointed (black lines) sandstone, (b) ripple marks and (c) cross-stratification.

2. Materials and Methods:

The fieldwork of the Nari Nai Section has been conducted, where formation has fine exposure and displays its utmost lithological features. Nari Formation is 230m thick in the study section, measured by the Brunton and tape method and Jacob's staff method (Compton, 1962). Thirty-three lithological units were identified, and measured and the same number of samples (29 sandstone and 4 shale samples) were collected (Figure 2). Sixteen samples of sandstone were moderately to well compacted and suitable for thin section preparation while thirteen samples were friable to lose and not appropriate for petrography.

Standard Petrographic study of thin sections, X-Ray Diffraction (XRD), Scanning Electron Microscopy (SEM), and Energy Dispersive X-Ray Spectrometry (EDS) were carried out during the present study. All the equipment used during the present study is available at Advanced Research Laboratories, Centre for Pure and Applied Geology University of Sindh, Jamshoro, Pakistan. Before preparation of thin sections, samples were engrossed in blue dye for 24 hours for prominent detection of porosity in thin section. XRD analysis of these samples was carried out for specific qualitative and quantitative recognition of minerals and to aid petrographic study. Selected samples were grinded as powder, then sieved through mesh of 180 µm and 03 grams of sieved powder was taken for XRD. XRD was carried under Germany-based company Bruker AXS manufactured D8 Advance machine. XRD results were evaluated using the computer-based software "Eva". Ten well compacted and fine-grained samples were selected for SEM and EDS analysis. These samples were studied through SEM (model- JEOL JSM-6490LV) fixed with XFlash Detector 4010 energy dispersive X-ray analyzer (company-Bruker AXS) for determination of chemical composition. For porosity determination thin sections are point counted to evaluate porosity.

ArcGIS software is used for the preparation of a location map and geological map of the study area. The columnar section was prepared using log plot software. Picture marking and labeling were done using different software such as Canvas X, CorelDraw, Xara xtreme Pro and Adobe Photoshop.

3. Results and Discussion

3.1. Petrography

Petrography is carried out to understand the percentage of detrital grains, matrix, cement and porosity in the studied sediments. The results of petrography are tabulated in Table 2. Quartz is the most dominant detrital grain observed during petrography ranging between 66-85%. The studied samples contain varying amounts of matrix between 5-26%. Broken quartz fragments and clay minerals constitute the matrix.

3.1.1. Cementation

Iron oxide is the most dominant cement, and it is identified in every studied sample. The sandstone of some of the samples is highly oxidized, where iron oxide forms a continuous network and quartz mineral gains are immersed in it (Figure 4a). It indicates the prolonged sub-areal exposure of the wet sediment surface containing abundant iron-bearing minerals. In some samples, the iron oxide cement occurs as isolated patches or black outline cover around quartz grains. Well lithified and compacted samples of sandstone contain more iron oxide (Figure 4a), than friable to moderately lithified samples (Figure 4e). Calcite is the second dominant cement that is observed in eight studied samples and occurs as inter-granular void-filling cement (Figure 4b). Dolomite is the third dominant cement and is found in five of sixteen studied samples. Dolomite generally occurs as patchy and irregular (Figure 4c). Some samples contain both iron oxide and calcite or iron oxide and dolomite cement (Figure 4b-c). Calcite cement is generally observed in samples of the lower part of the formation (Table 1). Dolomite cement is rarely reported previously, but iron oxide and calcite cement from the Nari Formation are reported

Table 2: Petrographic data of sandstone of Nari Formation from Nari Nai Section, showing the counted percentage of detrital grains, matrix, cement, and porosity (MCP=Mean Counted Porosity).

S. No.	Sample No.	Detrital Grains (%)	Matrix (%)	Cement (%)				MCP %	Total %
				Iron Oxide	Calcite	Dolomite	Silica		
1	NR-2	78	8	5	1	4	0	4	100
2	NR-5	73	6	2	0	1	0	18	100
3	NR-6	80	5	6	8	0	0	1	100
4	NR-8	76	10	10	1	0	0	3	100
5	NR-9	70	17	11	1	0	0	1	100
6	NR-11	76	10	1	8	0	0	5	100
7	NR-12	80	7	3	1	1	0	8	100
8	NR-14	78	12	4	1	1	0	4	100
9	NR-16	85	5	2	0	0	2	6	100
10	NR-18	82	10	2	0	0	1	5	100
11	NR-19	80	12	3	0	0	1	4	100
12	NR-24	73	8	2	1	0	0	16	100
13	NR-25	75	16	8	0	0	0	1	100
14	NR-28	72	18	2	0	4	1	3	100
15	NR-30	66	26	3	0	0	1	4	100
16	NR-31	70	20	3	0	0	0	7	100

different localities of the Southern Indus Basin (Mahmud and Sheikh, 2009; Ahmed et al., 2020; Shar et al., 2021a).

3.1.2. Compaction

In terms of compaction, long contacts are very dominant and were observed in twelve of sixteen studied samples. Point contacts are the second-most dominant type of contacts. They are observed in eleven samples, but their relative concentration is less than long contacts. Non-contacts are present in seven studied samples. Occasionally concave-convex contacts are also observed from some samples of lower part of the Nari Formation (Figure 4 d-e). The nature of grain contacts within the sandstone of the Nari Formation has not previously reported, however, mechanical compaction been reported (Shar et al., 2021b).

3.1.3. Dissolution and Overgrowth

Dissolution and overgrowth of quartz are also observed in samples of the Nari Formation. Quartz dissolution is common in well-cemented sandstone and it is observed in 8 out of 16 samples. Where quartz is dissolved, it is later filled with cement (Figure 4f). Quartz overgrowth can be seen in those samples where some pore spaces are preserved and not destroyed by any cement (Figure 4g). Quartz overgrowth is observed in 5 out of 16 samples. Dissolution of different framework grains, such as quartz and feldspar was earlier reported (Shar et al., 2021b), however, quartz overgrowths are only reported during this work.

3.1.4. Grain Fracturing

Fractured mineral grains are observed in 5 out of 16 samples (Figure 4h). Fracturing of framework mineral grains from the Nari Formation are previously reported (Mahmud and Sheikh, 2009; Ahmed et al., 2020; Paryal et al., 2020; Shar et al., 2021a; Shar et al., 2021b).

3.1.5. Porosity

The fine-grained and oxidized sandstone of the Nari Formation contains negligible porosity (Figure 4a). Medium-grained, poorly cemented sandstone contains significant effective porosity, which ranges up to 18% (Figure 4e). The point counting average of porosity is shown in Table 2. Eleven studied samples have 1 to 5% isolated porosity (Figure 4i). Five samples contain 6 to 18% effective porosity (Figure 4d, e, g). Those thirteen samples which were friable to lose and not studied under petrography contain more porosity than the studied samples. Therefore, it is clear that eighteen out of twenty-nine samples of sandstone contain effective porosity, which would prove good reservoir horizons. Eleven of twenty-nine samples contain 1 to 5% isolated porosity. Primary porosity is prone to destruction due to cementation and compaction. Primary porosity and permeability of the Nari Formation are reduced by diagenesis from the Jamshoro area of the Karachi arc as reported by Shar et al. (2021a).

3.2 XRD Analysis

Petrography is supported with XRD analysis. This practice is employed to recognize different minerals. This study also aided in the confirmation of minerals, which were identified during petrography. Iron oxide is the dominant cementing material observed in petrography, which is not recognized by XRD due to its amorphous nature.

XRD results displayed that quartz is an abundant framework mineral, and it ranges from 88% (Figure 5a) to 100% (Table 3). Calcite is identified in seven samples and it ranges from 1-10% (Figure 5a-b). Dolomite is detected in five samples and it ranges from 1-5% (Figure 5a, c). Clay minerals are identified by XRD in four samples. Kaolinite is identified in three samples, ranging from 5-8% (Figure 5a, d) and Illite is identified in two samples (Figure 5a). Minerals observed during XRD and their respective percentage are tabulated in Table 3.

3.3 SEM and EDS Analysis

Iron oxide is the most abundant cement observed during SEM. It forms a continuous medium of cement in which framework minerals can be identified either partially or completely submerged (Figure 6a). It is also observed as scattered grains in poorly cemented samples (Figure 6b). Calcite is observed as scattered patches (Figure 6c) as well as forming poikilotopic cement in which quartz grains are surrounded (Figure 6d). Grain contacts are hard to identify in highly cemented samples, but long contacts (Figure 6b-c), point contacts, and non-contacts (Fig. 6c-d) are observed in some samples.

EDS analysis of selected samples is carried out for the precise identification of framework minerals and various types of cements. Quartz is the dominant framework mineral present in studied samples. Peaks of silicon and oxygen indicate the presence of quartz (Figure 7a). Iron is recognized by EDS in all studied samples that range from 2-12% (Figure 7a). Calcium is part of calcite and is detected in eight samples (Figure 7b). Higher peaks of both calcium and magnesium are observed in some samples along with peaks of silicon and oxygen indicating the presence of dolomite in these samples (Figure 7c).

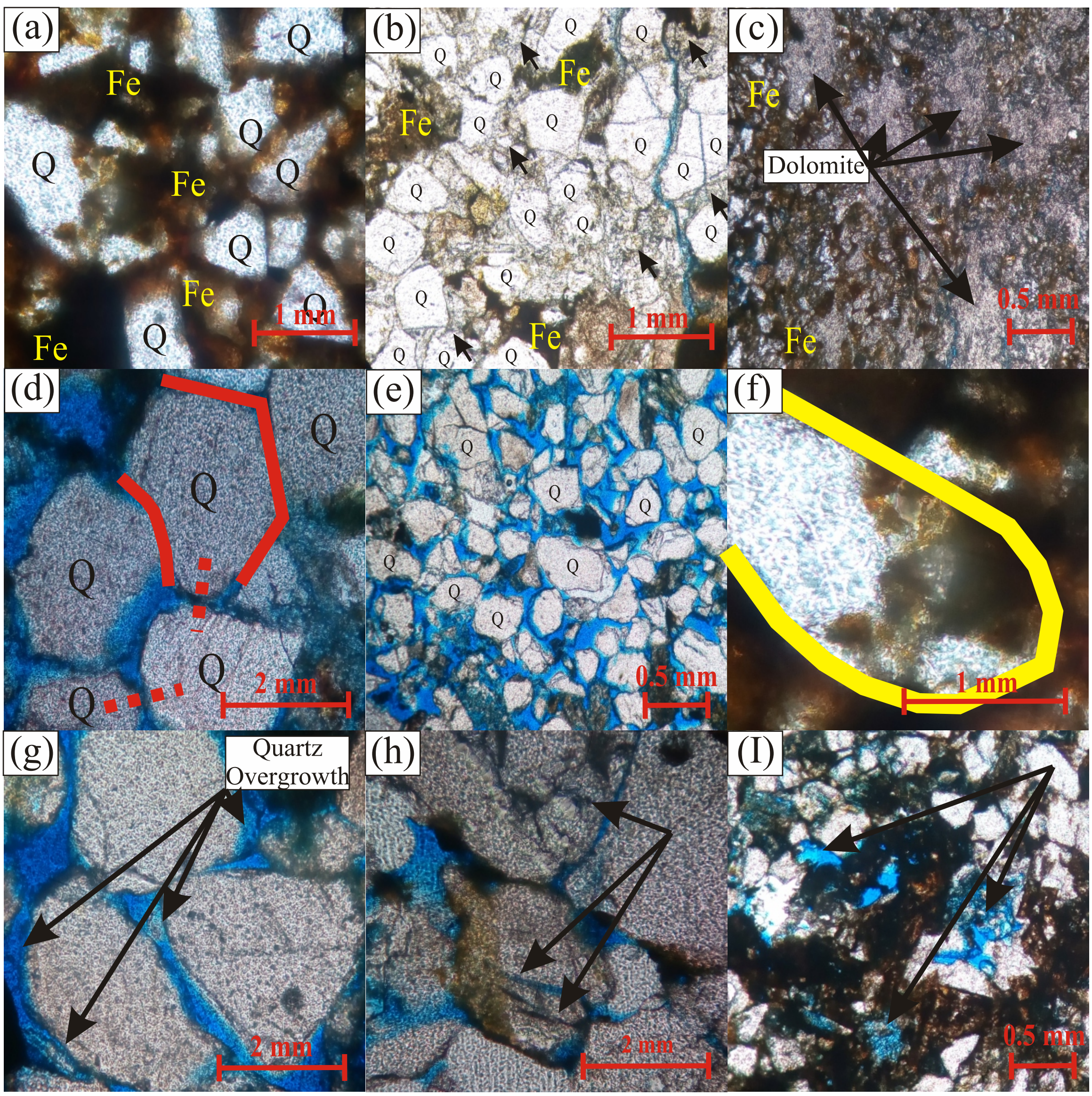

Fig. 4 (a-i): Petrographic photomicrographs showing (a) Iron oxide cement {Fe}, {Q=Quartz}; (b) calcite cement {arrows}; (c) patches of dolomite cement; (d) concavo-convex contacts {arc line}, long contacts {straight lines} and point contacts {dotted lines}; (e) non-contacts and effective porosity {blue color}; (f) dissolved quartz grains outlined yellow; (g) quartz overgrowths; (h) fractured quartz grains; (i) isolated porosity.

Table 3: Percentage of mineral composition of sandstone of Nari Formation from Nari Nai Section, observed during petrography and XRD method.

S. No.	Sample No.	Percentage of detected minerals				
		Quartz (88-100%)	Calcite (1-10%)	Dolomite (1-5%)	Kaolinite (3-7%)	Illite (5-8%)
1	NR-2	94	1	5		
2	NR-5	100				
3	NR-6	90	10			
4	NR-8	100				
5	NR-9	88	1	1	5	5
6	NR-11	88	9		3	
7	NR-12	96	2	2		
8	NR-14	97	1	2		
9	NR-16	100				
10	NR-18	100				
11	NR-19	92			8	
12	NR-24	98	2			
13	NR-25	92				8
14	NR-28	97		3		
15	NR-30	100				
16	NR-31	100				

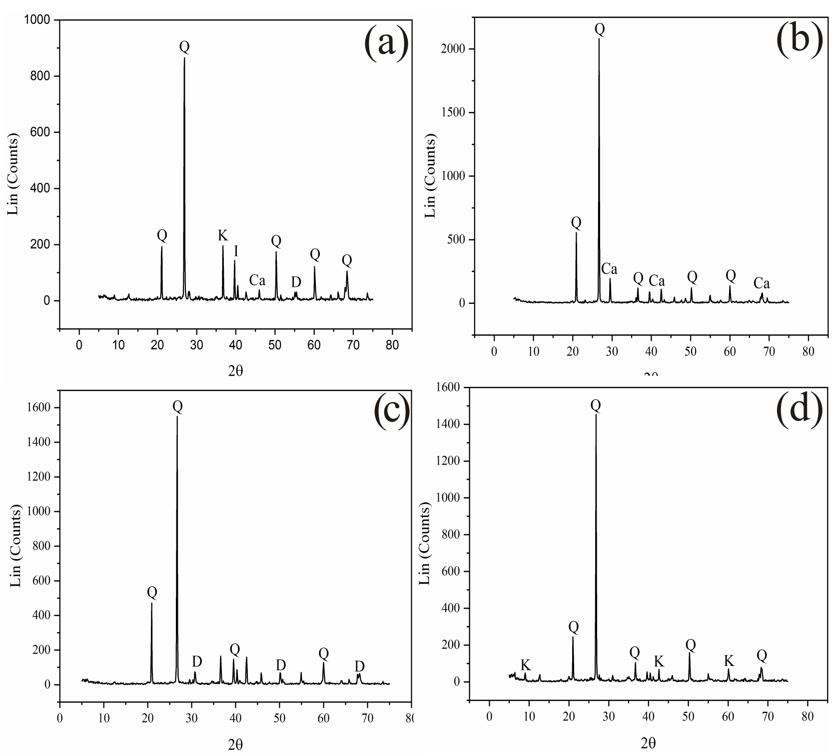

Fig. 5: X-ray diffractograms showing different detected minerals in the sandstone of the Nari Formation (Q=Quartz; K=Kaolinite; I=Illite; D=Dolomite; Ca=Calcite).

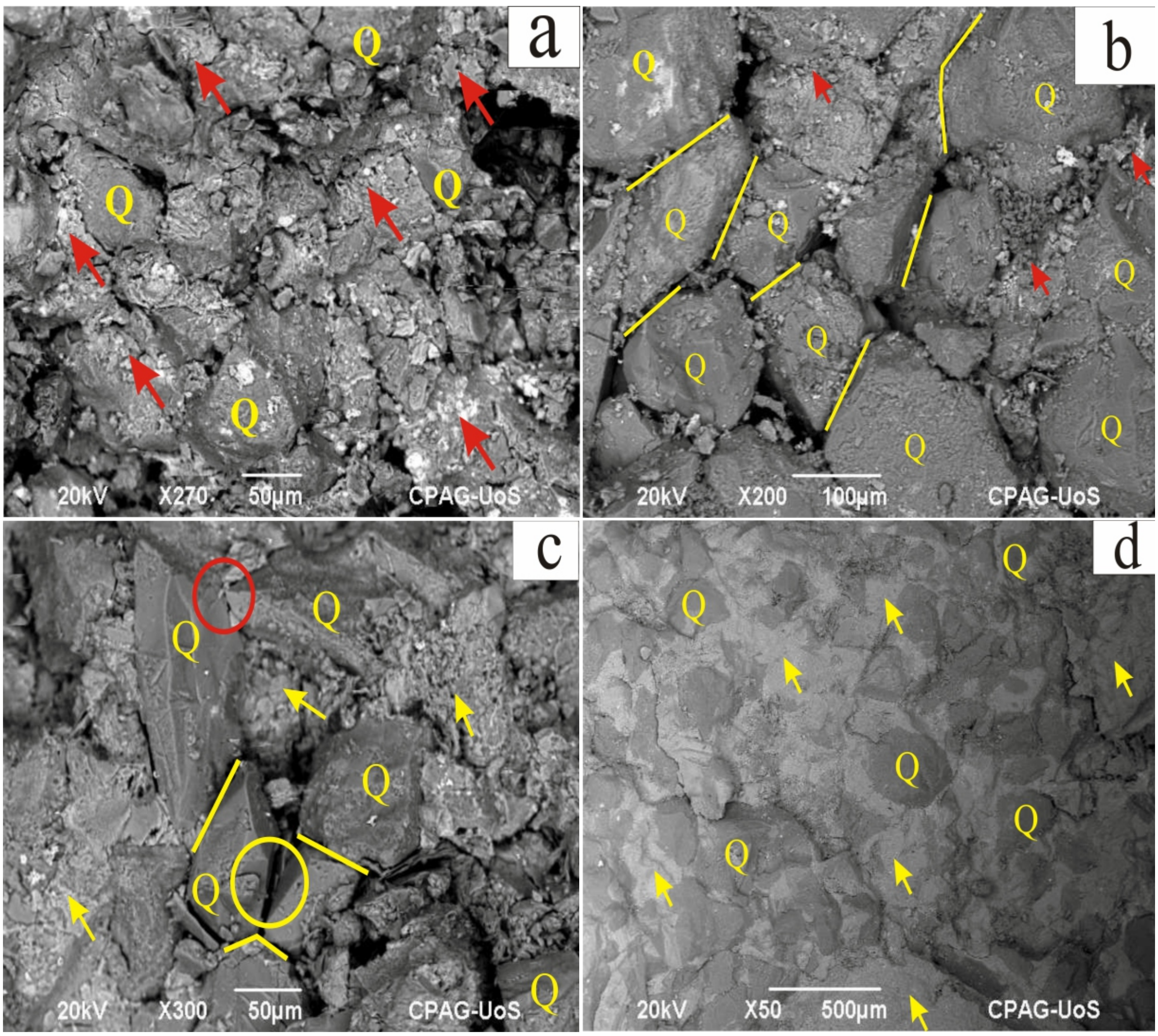

Fig. 6 (a-d): SEM micrographs, showing different diagenetic features, such as iron oxide (red arrows) and calcite (yellow arrows) cements, grain contacts (yellow lines and circles).

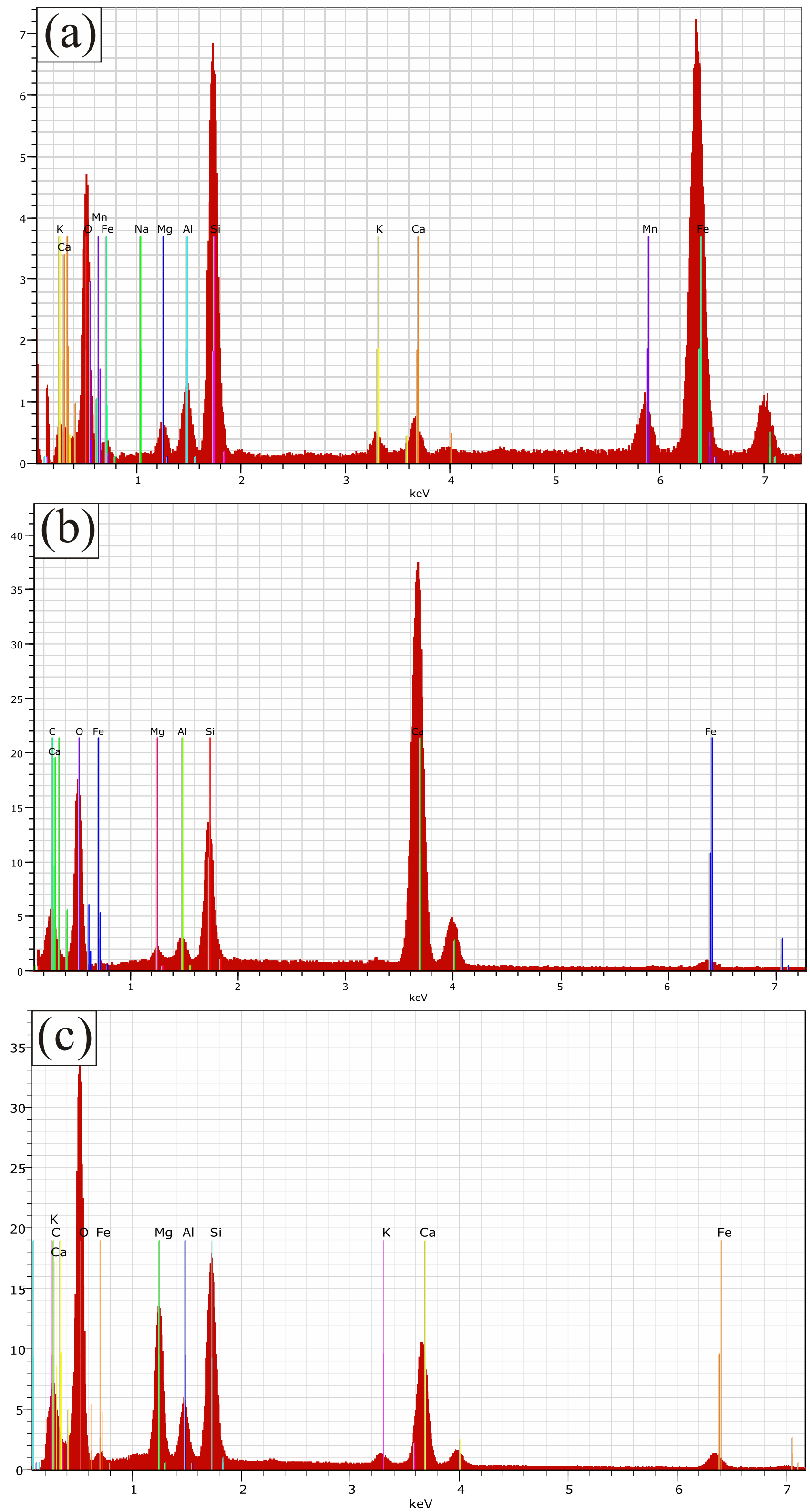

Fig. 7 (a-c): EDS point analysis graphs showing the elemental distribution of selected framework minerals and cementing material.

3.4 Diagenesis of Nari Formation

Diagenetic episodes of sandstone of the Nari Formation could be classified into three stages, which are eogenesis, mesogenesis, and telogenesis. Table 4 shows the inferred paragenic succession of the major diagenetic processes that operated on the sandstone.

3.4.1. Eogenesis

Eogenesis of the Nari Formation started during the Oligocene, soon after the starting of the deposition. The exact duration of eogenesis of the Nari Formation is not exactly known, but the conformable thickness of overlying strata and the present geothermal gradient of the study area indicates that the eogenesis might have continued throughout the Oligocene and Miocene. This stage of the sandstone of the Nari Formation is controlled by a depositional environment under a temperature below 70ºC. In this stage chemical composition of pore water is generally influenced by the depositional sedimentary environment (Chapelle, 1993; Zhang et al., 2020; Qamar et al., 2023). All processes of this stage occurred at the interface of water-sediment or air-sediment or only a few meters below the surface of sediments after their deposition and before lithification. Observed processes in this stage are precipitation calcite iron oxide cementsand minor compaction.

Table 4: Paragenetic succession interpreted from petrography for the major diagenetic processes, which operated on the sandstone of the Nari Formation.

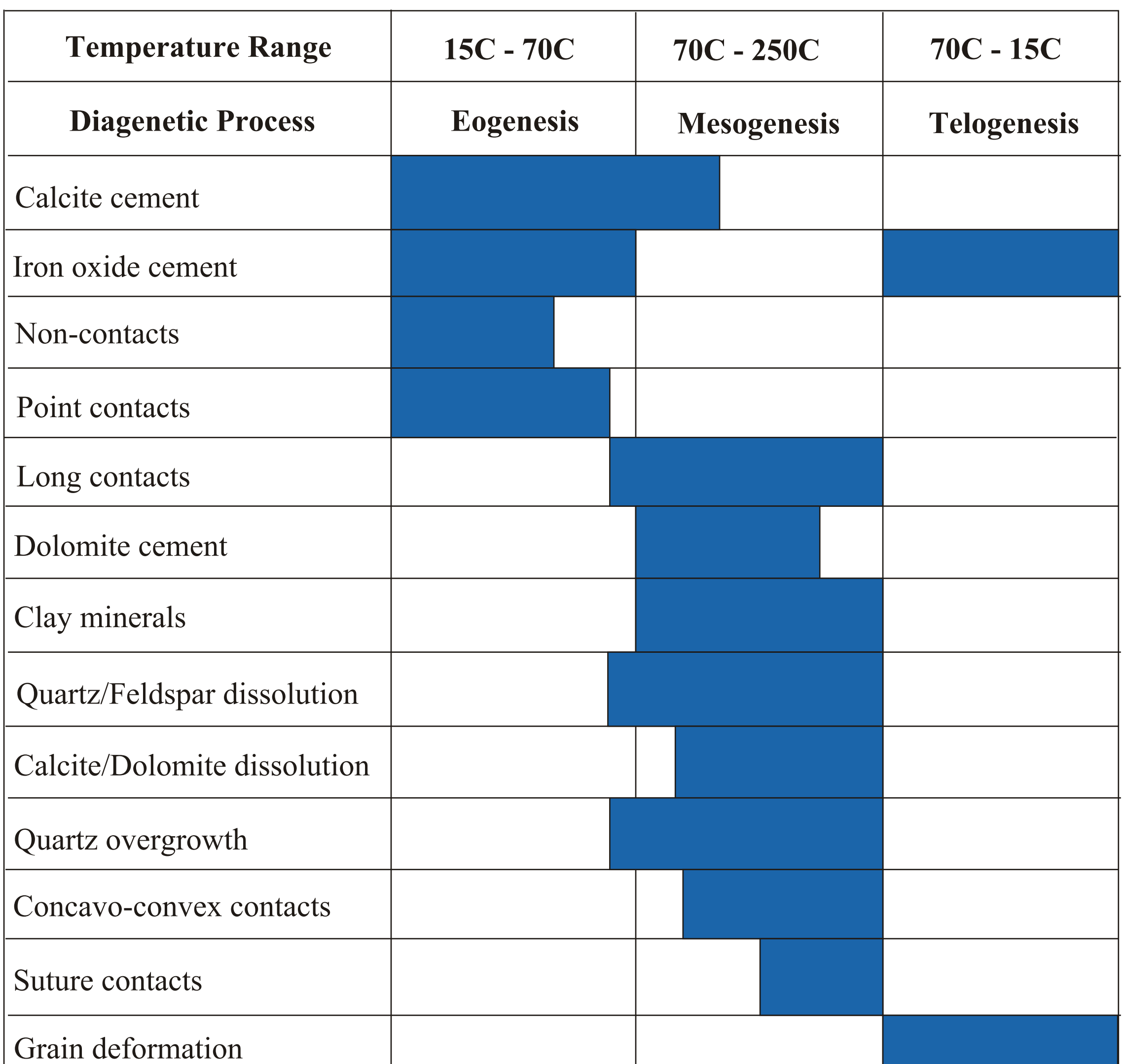

Calcite and iron oxide cement occurs in two modes, first is a continuous framework of cement that surrounds framework minerals, also called poikilotopic cement, and the other mode is dispersed grains of these cements. Continued framework of calcite and iron oxide cement observed in samples indicates that they are developed in eogenesis, where there is an abundant supply of the sources of these cement. Poikilotopic cement is only observed in eogenesis (Boggs, 2009). Precipitation of calcite requires warm alkaline water rich in calcium-bearing minerals such as calcite and aragonite. This condition stands in good agreement with waters of tropical oceans (Zhong and Mucci, 1989; Moore and Wade, 2013). The presence of calcite cement in the sandstone of the Nari Formation suggests that warm alkaline water was present in the Indus Basin during the Oligocene. The skeleton and shells of the majority of marine life are composed of aragonite, which is chief source of limestone and calcite cements in the sandstone. Precipitation of early poikilotopic calcite cement is related to the recrystallization of significant amounts of skeletal debris present at the time of deposition of sandstone (Imam and Shaw, 1985; Zhang et al., 2020; Zhang et al., 2022). Poikilotopic cement of calcite develops when sediments are loose, and there are sufficient intergranular spaces (Nichols, 2009). Warm and alkaline water also facilitates the dissolution of quartz and feldspar. Therefore, some quartz and feldspar grains might have dissolved during the eogenesis. However, early indications of quartz and feldspar dissolution could not be identified due to abundant cementation in eogenesis and telogenesis. Calcite cement developed during eogenesis was worked out by Zaid and Al Gahtani (2015) in the Triassic Hawkesbury Sandstone from the southern Sidney Basin of Australia. Baiyegunhi et al. (2017) also support the precipitation of carbonate cement during the eogenesis. Eogenetic calcite cement in the sandstone is also reported by Zhu et al. (2018) from the sandstone of the Upper Triassic Yanchang Formation of the Ordos Basin of China.

Iron oxide is the dominant cement observed in all studied samples of sandstone. Iron oxide cement represents the second phase of cementation during eogenesis because it corroded the calcite cement in some samples. It seems to be deposited on the calcite cement and quartz grains in some samples, which also confirms that it precipitated after the calcite cement. Iron in the depositional environment might have been brought by rivers as a weathering product of iron-rich rocks. Dissolution and alteration of mafic minerals such as hornblende, pyroxene, magnetite, and biotite are the most presumed sources of iron (Walker, 1974; Rudmin et al., 2022). These minerals are mostly found in basic igneous rocks. Outcrops of ophiolites in Balochistan could be a source of this iron. Furthermore, oxidizing conditions in the depositional environment must have persisted during this stage to allow the development of iron oxide (Schmidt and McDonald, 1979; Saha and Bhattacharya, 2022; Adamolekun et al., 2023). This indicates that the development of iron oxide occurred during eogenesis. Precipitation of calcite cement is the indication of a marine environment, while iron oxide indicates the oxidizing sub-areal environment. The presence of both types of cement in the same units suggests the fluctuating sea water during the time of sandstone deposition. This fact establishes that the sandstone of the Nari Formation is deposited in the tide-dominated shallow clastic depositional setting. The presence of ripple marks and cross stratification also indicates the tide-dominated depositional environment. The massive sandstone of the Nari Formation is usually cliff-forming. According to Nichols (2009), massive cliff-forming sandstone is deposited on the shoreface of a tide-dominated shallow sea.

Precipitation of iron oxide or iron-bearing minerals such as hematite and pyrite as cement during the eogenesis is also supported by Gier et al. (2008); Zaid and Al Gahtani (2015); and Chima et al. (2018). Gier et al. (2008) reported the eogenetic pyrite cement in the Miocene sandstone of marine origin from the Vienna Basin of Austria. Zaid and Al Gahtani (2015) proved the presence of eogenetic iron oxide cement in the Triassic Hawkesbury Sandstone from the southern Sidney Basin of Australia. Chima et al. (2018) reported the eogenetic iron oxide cement from the Triassic sandstones of the Stromberg Group of the Eastern Cape province of South Africa.

Floating grains in cement and grains with non-contacts and point contacts are observed as indications of minor compaction in the early stage of diagenesis. Compaction is rarely observed in eogenesis due to a lack of overburden. Cementation even further reduces the compaction effects (Boggs, 2009; Nichols, 2009). In the global research on diagenesis, little attention is paid to the nature of grain contacts developed during the eogenesis. This is because there are scant prospects of preservation of epigenetic contacts. With the increase of burial and overburden, grain contacts progressively change from non-contact to point contact, from point contact to long contact and from long contact to concavo-convex contact. Concave-convex contacts become suture contacts in extreme diagenetic environments (Baiyegunhi et al., 2017; Chima et al., 2018; Baiyegunhi et al., 2020).

3.4.2 Mesogenesis

Heavy influx of sediments from rising mountain ranges deposited during the Miocene and Pliocene brought the Nari Formation into the realm of mesogenesis. If the thickness of the conformable overlying sequence and the geothermal gradient of that area are known, then the diagenetic stage of the underlying sequence during a particular geological time can be determined. Determination of the diagenetic stage during a particular geological time would help to correlate the diagenesis, tectonics, and basin evolution. The conformable thickness of the Miocene and Pliocene sequence in the Kirthar Range, Pakistan is more than 2000 m (Shah, 2009) and the geothermal gradient in the study area is 3.5ºC/100m (Bender and Raza, 1995). Therefore, it can be calculated that, by the end of the Pliocene base of the Nari Formation would be at depth of about 2500m and a temperature of more than 70ºC. Both these conditions of depth and temperature belong to mesogenesis (Worden and Burley, 2003; Boggs, 2009). It suggests that by the end of the Pliocene, Nari Formation was experiencing mesogenesis. Kirthar Foredeep, a least deformed tectonic entity of the Southern Indus Basin is located in the east of Kirthar Range (Figure 1a). The top and bottom of the Nari Formation are encountered between the depths of 1500s to 2500m respectively in the wells drilled in the Kirthar Foredeep. In the foredeep region, Nari Formation is still in the regime of mesogenesis. This stage covers all the changes that sandstone of Nari Formation underwent during and after lithification and before tectonic deformation and uplifting. This regime of diagenesis is characterized by a temperature range between 70ºC to 250ºC, an increase in overburden pressure due to burial under successive layers of sediments, and a change in pore water chemistry (Worden and Burley, 2003; Boggs, 2009). Observed processes of this stage are continued cementation of calcite, precipitation of dolomite and clay mineral cement, dissolution of quartz, development of quartz overgrowth and compaction.

Calcite and dolomite cement in poor to moderately-compacted sandstone of the Nari Formation occur as dispersed patches between the grains. This shows that they are precipitated in the preserved pore spaces after sufficient compaction. The source of scattered calcite and dolomite cement is connate alkaline water containing calcium-bearing minerals. Poor mesogenic carbonate cementation suggests a lesser concentration of calcium-bearing minerals in the connate water than that in the depositional water. Unstable clastic grains release cations to connate water, which allows the precipitation of calcite and dolomite cement in voids or replaces mineral grains during myogenesis (Baiyegunhi et al., 2017). According to Boggs (2009), dolomite cement only precipitates in the mesogenesis.

Kaolinite and Illite are the clay minerals present in some sandstone horizons of the Nari Formation. Clay minerals detected during XRD analysis are formed during mesogenesis due to the breakdown of weaker lithic fragments such as feldspar, and recrystallization of other clay minerals (Nichols, 2009). Kaolinite and Illite developed during the mesogenesis are reported by different workers across the world in the sandstone of different ages. For example, Chima et al. (2018) reported the mesogenetic kaolinite and illite from the Triassic sandstones of the Stromberg Group of the Eastern Cape province of South Africa. Mesogenetic Kaolinite and Illite in the sandstone are also reported by Zhu et al. (2018) from sandstone reservoir of the Upper Triassic Yanchang Formation of the Ordos Basin of China.

During petrography dissolution of whole quartz grains as well as dissolution limited at grain contacts (pressure dissolution) is observed. Pressure dissolution indicates the deeper burial of sediments under a thick pile of overlying sediments. Under such conditions increased temperature and overburden pressure accompanied by pore water, quartz dissolved along its margins. This is because maximum stress is directed along the margins of quartz (Nichols, 2009). The dissolution of quartz occurs due to warm alkaline pore water under mesogenetic realm (Nichols, 2009; Boggs, 2009). Pressure dissolution of quartz resulted in concavo-convex and suture contacts as observed during petrography. Silica released due to quartz dissolution is deposited in empty pore spaces as quartz overgrowth at temperatures about 70ºC to 90ºC after sufficient compaction of sandstone (Baiyegunhi et al., 2017). The temperature range of 70ºC to 90ºC marks the early phase of mesogenesis. Precipitation of silica as quartz overgrowth requires relatively cooler and slightly acidic pore water saturated with silica (Nichols, 2009). Cooler and acidic connate water also facilitates the dissolution of calcite and dolomite. Therefore, quartz overgrowths are observed in those sediments, where calcite or dolomite are scarce or absent. It is worth mentioning here that warm alkaline pore water rich in K, Si, and Al are ideal for the formation of illite and dissolution of quartz (Baiyegunhi et al., 2017). Slightly acidic pore water is ideal for the kaolinite formation and precipitation of quartz overgrowth (Nichols, 2009; Baiyegunhi et al., 2017). Therefore, the precipitation of carbonate cement, quartz dissolution, and Illite formation could be attributed as simultaneous processes during the mesogenesis and same is true for the precipitation of quartz overgrowth, dissolution of carbonate cement, and kaolinite formation. The presence of both alkaline and acidic pore water during the mesogenesis is poorly understood.

Both the physical and chemical compaction is observed during petrography. Compaction is revealed by contacts of mineral grains (Taylor, 1950; Nichols, 2009). Chemical compaction is due to pressure dissolution, which results in concavo-convex and suture contacts (Boggs, 2009; Nichols, 2009). Physical compaction of sediments of Nari Formation continued during mesogenesis due to the increase in overburden pressure. This increased tightening of grains and decrease in porosity. Signatures of physical compaction during mesogenesis are point and long contacts of minerals grains observed during petrography and SEM. Little overburden pressure will result in point contacts while significant compaction will result in long contacts (Nichols, 2009). The sandstones of Nari Formation were subjected moderate to well mechanical compaction in lower part during its progressive burial as exhibited by grain contacts. Field observations also indicate the sandstone of particularly lower part of the Nari Formation is well compacted, lithified and hard. Generally upper part of the Nari Formation was found to be less compacted because concentration of long contacts was smaller than point contacts and non-contacts. Field observations also indicate that sandstone of upper part is generally moderately compacted to friable.

3.4.3. Telogenesis

The Pliocene-Pleistocene was the pinnacle of the tectonic deformation and uplifting of the western mountains of Pakistan (Auden, 1974; Schelling, 1999; Hinsch et al., 2019). The Pliocene-Pleistocene deformation brought the Nari Formation about 2000m above its place of deposition and exposed it for telogenesis. This uplifting brought the sandstone to the oxidizing environment, hence iron oxide precipitated during the telogenesis. Dissolved quartz grains are replaced by iron oxide indicating the oxidation during the telogenesis (Figure 4f). Indications of the telogenesis observed during fieldwork and also petrography are the presence of joints and fractured quartz grains respectively. Fracturing and deformation of mineral grains is also a process of mesogenesis as well. Fractures formed during mesogenesis are later generally filled by cement or other minerals, but telogenetic fractures are not filled with any mineral and remain empty in the form of secondary porosity (Selley, 1998; Bilal et al., 2022; Bello et al., 2022).

3.5 Regional Tectonic and Diagenetic Correlation

Oligocene inhabits imperative pose in the global tectonic framework in general and regional tectonic framework in particular. In a regional outlook from the Zagros Fold Belt of Iran to the Eastern Fold Belt of Bangladesh through Pakistan and China, different depositional, diagenetic, and tectonic realms existed during and after the Oligocene. Zagros Fold Belt and Kirthar Fold Belt are the continuation of Alpine-Himalayan Orogen. But unlike Kirthar Fold Belt, carbonate-evaporite-containing Asmari Formation was deposited in the Zagros Fold Belt area of the Iran during Oligocene-Miocene (Nader et al., 2009; Bigi et al., 2018). Both the Nari Formation of Pakistan and the Asmari Formation of Iran and Middle-East were deposited in the same realm of Neo-Tethys on the passive margins of their respective tectonic plates during the compressional episode (Raza et al., 1990; Bender, 1995; Molinaro et al., 2005; Hakro et al., 2021). Oligocene-Miocene Surma Group of the Eastern Fold Belt of Bangladesh is also a well-known petroleum system (Farhaduzzaman et al., 2015). Oligocene tectonics facilitated the deposition of Jenum Shale in this area, which acts as source rock of the system. In Pakistan Oligocene rocks exist only in the Kirthar and Suleiman ranges. Due to the uplifting of Himalaya-Tibet and western mountain ranges of Pakistan, basin became restricted only to the foot-hills of Kirthar and Suleiman ranges (Raza et al., 1990) No Oligocene sequence exists in the foothills of Himalaya or the upper Indus Basin of Pakistan (Shah, 2009). Apart from the regions of fold belts in Pakistan, sandstone facies were also deposited in the intra-cratonic Xihu sag of the East China Sea Basin (Wang et al., 2021) and in the Mouth Basin of South China Sea during Oligocene (Wu et al., 2019) Sandstone of the Nari Formation of Kirthar Range, E_3H Formation of the Xihu sag of the East China Sea Basin and Zhuhai Formation of the Mouth Basin of South China Sea has only lithological and chronological similarities but having different tectonic, depositional as well as diagenetic histories. Therefore, their comparative study will help to understand the control of tectonics and depositional environment on the diagenesis. The sandstone of the Nari Formation was deposited on a colliding plate margin in a tide-dominated shallow sea. E_3H Formation was deposited during the period of compressional and inversion tectonics in a braided stream delta lake setting (Wang et al., 2021). Zhuhai Sandstone was deposited during the early period of post-rift stage during the extensional phase of tectonics. Zhuhai Sandstone was deposited in the fan delta to tidal flat depositional system (Wu et al., 2019). There are also diagenetic distinctions between Asmari Formation, Jenum Shale, E_3H Formation, Zhuhai Formation, and Nari Formation. All these formations experienced mesogenesis up to the late stage of diagenesis, except Nari Formation. The Nari Formation experienced mesogenesis. After experiencing mesogenesis, Nari Formation deformed and uplifted to the surface and experienced telogenesis. This deformation and uplifting of the Nari Formation occurred due to the climax episode of deformation in the Kirthar-Himalayan-Tibetan orogen during the Pliocene-Pleistocene (Royden and Clark, 2004). Neither of the other formations mentioned above underwent tectonic uplifting nor experienced telogenesis. The clastic Nari Formation of Kirthar Range, Pakistan has not yet proven as a successful reservoir rock, but on the other hand, carbonate-evaporite Asmari Formation of the Zagros Fold Belt, E_3H Formation of the Xihu sag of the East China Sea Basin and Zhuhai Sandstone of the Mouth Basin of South China Sea are proved excellent oil and gas reservoir rocks. Therefore, this fact can be established that it is the tectonics that dominantly controls the diagenetic stages of a formation, and hence its source and reservoir rock potential.

4. Conclusions

The present study has shown that the sandstone of Nari Formation from Nari Nai section, Kirthar Range, Pakistan experienced eogenesis, mesogenesis, and telogenesis. The diagenesis of the Nari Formation is controlled by Oligocene-Pleistocene depositional environment and tectonic events. The important processes of diagenesis, which affect the sandstone, are cementation, compaction, dissolution, alteration, quartz overgrowth and grain fracturing. During eogenesis, sandstone mainly underwent cementation and minor compaction. Compaction, dissolution, alteration, and quartz overgrowth are the major processes of mesogenesis. Grain fracturing and oxidation are the process of telogenesis. Iron oxide is the most abundant type of cement observed in all studied samples, followed by calcite and dolomite cement. Sandstone of Nari Formation subjected poor to well compaction as exhibited by grain contacts. Long contacts and point contacts are dominant and occasionally concavo-convex contacts, suture contacts and non-contacts of grains are observed. Primary porosity ranges between 1-18% in studied samples, while friable to poorly compacted sandstone is also present. Nari Formation is correlated with its chronostratigraphic equivalent formations in the region in terms of depositional environment, diagenesis, and tectonics. It is concluded that it is the tectonics that control the depositional environment, diagenesis, and hence hydrocarbon significance of the formation.

Authors Contribution

Surriya Bibi Ahmedani is corresponding author and contributed to the field data collection and petrography. She also arranged the paper as per JHES format. Muhammad Hassan Agheem supervised the field data collection and analyzed samples under XRD. Asghar A.A.D. Hakro conceptualized the work and wrote the "abstract", "materials and methods" and "conclusions" sections of the manuscript. Aijaz Ali Halepoto contributed the field data collection and SEM-EDS analysis in the laboratory. He wrote the "Introduction" section of this paper. Rafique Ahmed Lashari worked on and finalized the illustrations being used in this paper. The idea of regional correlation was contributed by Ghulam Mustafa Thebo and he wrote the "regional tectonic and diagenetic correlation" section of the manuscript.

Acknowledgements

The authors pay gratitude to the University of Sindh, Jamshoro, Pakistan for providing logistical support for this research. The authors also acknowledge to Mr. Muhammad Kashif Samoon, Assistant Professor at Centre for Pure and Applied Geology, University of Sindh, Jamshoro, Pakistan, for reserving his precious time for the SEM-EDS analysis at Advance Research Laboratories of Centre for Pure and Applied Geology, University of Sindh, Jamshoro. The authors are thankful to Mr. Muhammad Soomar Samtio, Lecturer at Centre for Pure and Applied Geology, University of Sindh, Jamshoro, Pakistan, for his valuable suggestions and discussions, which helped a lot to improve this work.

References

Adamolekun, O.J., Busch, B., Oluwajana, O.A., Suess, M.P., and Hilgers, C., 2023. Diagenetic evolution of continental to shallow marine Mesozoic--Cenozoic deposits, Eastern Dahomey Basin, Nigeria: Implications for reservoir quality. Zeitschrift Der Deutschen Gesellschaft Für Geowissenschaften (ZDGG) 174.

Ahmed, Z., Khan, A.S., and Ahmed, B., 2020. Sandstone Composition and Provenance of the Nari Formation, Central Kirthar Fold belt, Pakistan. Pakistan Journal of Geology, 4, 90–96. https://doi.org/10.2478/pjg-2020-0010

Ajdukiewicz, J.M., and Lander, R.H., 2010. Sandstone Reservoir Quality Prediction: The state of the art. American Association of Petroleum Geologist Bulletin, 94, 1083–1091.

Anees, A., Zhang, H., Ashraf, U., Wang, R., Thanh, H.V., Radwan, A.E., Ullah, J., Abbasi, G.R., Iqbal, I., and Ali, N., 2022. Sand-ratio distribution in an unconventional tight sandstone reservoir of Hangjinqi area, Ordos Basin: Acoustic impedance inversion-based reservoir quality prediction. Frontiers in Earth Science, 10, 1018105.

Ashraf, U., Zhang, H., Anees, A., Ali, M., Zhang, X., Shakeel Abbasi, S., and Nasir Mangi, H., 2020. Controls on reservoir heterogeneity of a shallow-marine reservoir in Sawan Gas Field, SE Pakistan: Implications for reservoir quality prediction using acoustic impedance inversion. Water, 12, 2972.

Auden, B.A., 1974. Afghanistan-west Pakistan. In: Spencer, A.M. (Ed.), Mesozoic-Orogenic Belts. Scottish Academic Press, Edinburgh, 235–253.

Baiyegunhi, C., Liu, K., and Gwavava, O., 2017. Diagenesis and Reservoir Properties of the Permian Ecca Group Sandstones and Mudrocks in the Eastern Cape Province, South Africa. Minerals, 7, 1–26. https://doi.org/10.3390/min7060088

Baiyegunhi, T.L., Liu, K., Gwavava, O., and Baiyegunhi, C., 2020. Impact of Diagenesis on the Reservoir Properties of the Cretaceous Sandstones in the Southern Bredasdorp Basin, Offshore South Africa. Minerals, 10, 1–33.

Bannert, D., Cheema, A., Ahmed, A., and Schaffer, U., 1992. The Structural Development of the Western Fold Belt, Pakistan. Geologisches Jahrbuch Reihe, B80, 3–60.

Bashir, A., Ali, M., Patil, S., Aljawad, M.S., Mahmoud, M., Al-Shehri, D., Hoteit, H., and Kamal, M.S., 2024. Comprehensive review of CO2 geological storage: Exploring principles, mechanisms, and prospects. Earth-Science Reviews, 249, 1–16. https://doi.org/10.1016/j.earscirev.2023.104672

Bello, A.M., Usman, M.B., Abubakar, U., Al-Ramadan, K., Babalola, L.O., Amao, A.O., Yandoka, B.M.S., Kachalla, A., Kwami, I.A., and Ismail, M.A., 2022. Role of diagenetic alterations on porosity evolution in the cretaceous (Albian-Aptian) Bima Sandstone, a case study from the Northern Benue Trough, NE Nigeria. Marine and Petroleum Geology, 145, 105851.

Bender, F.K., 1995. Paleogeographic and Geodynamic Evolution. In: Bender, F.K., Raza, H.A. (Eds.), Geology of Pakistan. Gebruder Borntraeger, 162–181.

Bender, F.K., and Raza, H.A. (Eds.), 1995. Geology of Pakistan. Gebruder Borntraeger.

Bickle, M.J., 2009. Geological carbon storage. Nature Geoscience 2, 815–818. https://doi.org/10.1038/ngeo687

Bigi, S., Carminati, E., Aldega, L., Trippetta, F., Kavoosi, M.A., 2018. Zagros fold and thrust belt in the Fars province (Iran) I: Control of thickness/rheology of sediments and pre-thrusting tectonics on structural style and shortening. Marine and Petroleum Geology 91, 211–224. https://doi.org/10.1016/j.marpetgeo.2018.01.005

Bilal, A., Yang, R., Fan, A., Mughal, M.S., Li, Y., Basharat, M., and Farooq, M., 2022. Petrofacies and diagenesis of Thanetian Lockhart Limestone in the Upper Indus Basin (Pakistan): Implications for the Ceno-Tethys Ocean. Carbonates and Evaporites, 37, 78.

Bjorlykke, K., 1988. Diagenesis. In: Chilingarian, G.V., Wolf, K.H. (Eds.),

Bloch, S., Lander, R.H., Bonell, L., 2002. Anomalously high porosity and permeability in deeply buried sandstones reservoirs. Origin and predictability. American Association of Petroleum Geologist Bulletin, 86, 301–328.

Boggs, S., 2009. Petrology of Sedimentary Rocks. Cambridge University Press, Cambridge. https://doi.org/10.1017/CBO9780511626487.

Chapelle, F.H., 1993. Ground-Water Microbiology and Geochemistry. John Wiley and Sons, New York.

Cheema, M.R., Ahmed, H., and Raza, S.M., 2009. Cenozoic. In: Shah, S.M.I. (Ed.), Stratigraphy of Pakistan. Geological Survey of Pakistan, 237–308.

Chen, B., Harp, D.R., Zhang, Y., Oldenburg, C.M., and Pawar, R.J., 2023. Dynamic risk assessment for geologic CO2 sequestration. Gondwana Research 122, 232–242. https://doi.org/10.1016/j.gr.2022.08.002

Chima, P., Baiyegunhi, C., Liu, K., and Gwavava, O., 2018. Diagenesis and rock properties of sandstones from the Stormberg Group, Karoo Supergroup in the Eastern Cape Province of South Africa. Open Geosciences, 10, 740–771. https://doi.org/10.1515/geo-2018-0059

Compton, R.R., 1962. Manual of Field Geology. John Wiley and Sons, New York.

Dar, Q.U.Z.Z., Pu, R., Baiyegunhi, C., Shabeer, G., Ali, R.I., Ashraf, U., Sajid, Z., and Mehmood, M., 2022. The impact of diagenesis on the reservoir quality of the early Cretaceous Lower Goru sandstones in the Lower Indus Basin, Pakistan.

Journal of Petroleum Exploration and Production Technology, 1–16.
Dars, H., Agheem, M.H., Solangi, S.H., Markhand, A.H., Sahito, A.G., Khokhar, Q.D., Thebo, G.M., and Shaikh, S.A., 2020. Effects of Diagenesis on the Reservoir Quality in the Upper Sands of Lower Goru Formation, Badin Block, Lower Indus Basin, Pakistan. International Journal of Economic and Environmental Geology, 11, 22–30.
Ding, L., Qasim, M., Jadoon, I.A.K., Khan, M.A., Xu, Q., Cai, F., Wang, H., Baral, U., and Yue, Y., 2016. The India–Asia collision in north Pakistan: Insight from the U–Pb detrital zircon provenance of Cenozoic foreland basin. Earth and Planetary Science Letters, 455, 49–61. https://doi.org/10.1016/j.epsl.2016.09.003
Duncan, P.M., and Sladen, W.P., 1884. Tertiary and Upper Cretaceous fossils of western Sind; Fasc. 4, the fossil Echinoidea from the Nari Series, the Oligocene formation of western Sind. Geological Survey of India Memoir Paleontology Indica, Series, 14 (1), 242–272.
Farhaduzzaman, M., Islam, M.A., Abdullah, W.H., and Islam, M.S., 2015. Petrography and Diagenesis of the Tertiary Surma Group Reservoir Sandstones, Bengal Basin, Bangladesh. Universal Journal of Geoscience, 3, 103–117. https://doi.org/10.13189/ujg.2015.030304
Ghani, H., Hinsch, R., Sobel, E.R., and Glodny, J., 2023. Oligocene to Pliocene structural evolution of the frontal Kirthar fold and thrust belt of Pakistan. Journal of Structural Geology, 176, 1–10. https://doi.org/10.1016/j.jsg.2023.104961
Gier, S., Worden, R.H., Johns, W.D., and Kurzweil, H., 2008. Diagenesis and reservoir quality of Miocene sandstones in the Vienna Basin, Austria. Marine and Petroleum Geology, 25, 681–695. https://doi.org/10.1016/j.marpetgeo.2008.06.001
Hakro, A.A.A.D., Samtio, M.S., Rajper, R.H., and Mastoi, A.S., 2022. Major Elements of Nari Formation Sandstone from Jungshahi Area of Southern Indus Basin, Pakistan. Pakistan Journal of Scientific and Industrial Research Series A: Physical Sciences, 65A, 248–259.
Hakro, A.A.A.D., Xiao, W., Mastoi, A.S., Yan, Z., Samtio, M.S., and Rajper, R.H., 2021. Grain size analysis of the Oligocene Nari Formation sandstone in the Laki Range, southern Indus Basin, Pakistan: Implications for depositional setting. Geological Journal, 56, 5440–5451. https://doi.org/10.1002/gj.4251
Halepoto, A.A., Agheem, M.H., Lashari, R.A., Hakro, A.A.A.D., and Ahmeda, 2023. Development and Synclinal-Anticlinal Breakthrough of Fault-Propagation Fold: Insights from Borr Dhoro Section of the Ranikot Anticline, Southern Kirthar Fold Belt, Pakistan. Sindh University Research Journal (Science Series), 55, 32–41. https://doi.org/https://doi.org/10.26692/surj-ss.v55i01.4179
Halepoto, A.A., Agheem, M.H., Wahid, S., Hakro, A.A.A.D., Lashari, R.A., and Ahmedani, S.B., 2022. Structural Analysis of the Ranikot Anticline, Southern Kirthar Fold Belt, Pakistan. Sindh University Research Journal (Science Series), 54, 21–27. https://doi.org/https://doi.org/10.26692/surj-ss.v54i04.4350
Hansen, H.N., Haile, B.G., Müller, R., and Jahren, J., 2023. New direction for regional reservoir quality prediction using machine learning-Example from the Stø Formation, SW Barents Sea, Norway. Journal of Petroleum Science and Engineering, 220, 111149.
Hinsch, R., Asmar, C., Nasim, M., Abbas, M.A., and Sultan, S., 2019. Linked thick-to thin-skinned inversion in the central Kirthar Fold Belt of Pakistan. Solid Earth, 10, 425–446. https://doi.org/10.5194/se-10-425-2019
Honarmand, J., and Amini, A., 2012. Diagenetic processes and reservoir properties in the ooid grainstones of the Asmari Formation, Cheshmeh Khush Oil Field, SW Iran. Journal of Petroleum Science and Engineering, 81, 70–79. https://doi.org/10.1016/j.petrol.2011.12.022
Hunting Survey Corporation, 1960. Reconnaissance Geology of Part of West Pakistan. A Colombo Plan Co-operative Project, Toronto, Canada.
Imam, M.B., and Shaw, H.E., 1985. The

diagenesis of Neogene clastic sediments from the Bengal Basin, Bangladesh. Journal of Sedimentary Petrology, 55, 665–671.

Jadoon, I.A.K., Ding, L., Nazir, J., Idrees, M., and Jadoon, S. ur R.K., 2020. Structural interpretation of frontal folds and hydrocarbon exploration, western sulaiman fold belt, Pakistan. Marine and Petroleum Geology, 117, 104380. https://doi.org/10.1016/j.marpetgeo.2020.104380

Jadoon, S.-R.K., Ding, L., Jadoon, I.A.K., Nazir, J., and Ping, F., 2024. Seismic data, cross-section balancing, and hydrocarbon prospectivity of the western Sulaiman fold belt, northwest Pakistan. Marine and Petroleum Geology, 160, 106644. https://doi.org/10.1016/j.marpetgeo.2023.106644

Kazmi, A.H., 1979. Active Fault Systems in Pakistan. In: Farah, A., De Jong, K.A. (Eds.), Geodynamics of Pakistan. Geological Survey of Pakistan, Quetta, 285–304.

Kazmi, A.H., Jan, M.Q., 1997. Geology and Tectonics of Pakistan. Graphic Publishers, Karachi.

Kazmi, A.H., and Rana, R.A., 1982. Tectonic Map of Pakistan.

Kelemen, P., Benson, S.M., Pilorgé, H., Psarras, P., and Wilcox, J., 2019. An Overview of the Status and Challenges of CO2 Storage in Minerals and Geological Formations. Frontiers in Climate, 1, 1–20. https://doi.org/10.3389/fclim.2019.00009

Khan, M.H., 1968. The dating and correlation of the Nari and Gaj formation. Geological Bulletin of Punjab University, 7, 57–65.

Khokhar, Q.D., Hakro, A.A.A.D., Solangi, S.H., Siddiqui, I., and Abbasi, S.A., 2016. Textural Evaluation of Nari Formation , Laki Range , Southern Indus Basin , Pakistan. Sindh University Research Journal (Science Series), 48, 633–638.

Mackenzie, F.T., 2005. Diagenesis and Sedimentary rocks. Treatise on Geochemistry. Elsevier: Oxford, UK., 446.

Mahmud, S.A., and Sheikh, S.A., 2009. Reservoir Potential of Lower Nari Sandstones (Early Oligocene) In Southern Indus Basin and Indus Offshore. SPE/PAPG Annual Technical Conference 50582.

Molinaro, M., Leturmy, P., Guezou, J.C., Frizon de Lamotte, D., and Eshraghi, S.A., 2005. The structure and kinematics of the southeastern Zagros fold-thrust belt, Iran: From thin-skinned to thick-skinned tectonics. Tectonics, 24, 1–19. https://doi.org/10.1029/2004TC001633

Moore, C.H., and Wade, W.J., 2013. Meteoric Diagenetic Environment. Developments in Sedimentology. Elsevier, 165–206.

Nader, F.H., Moradpour, M., Samani, P., Hamon, Y., Hosseiny, A., Daniel, J.M., Moallemi, A., and Pickard, N., 2009. Diagenesis of the Asmari Formation (Oligo-Miocene; SW Iran): Implications on Reservoir Modelling of a Giant Oilfield. 1st International Petroleum Conference and Exhibition, 4–9. https://doi.org/10.3997/2214-4609.20145905

Nichols, G., 2009. Sedimentology and Stratigraphy, 2nd ed. Wiley-Blackwell.

Paryal, M., Agheem, M.H., Hussain, G., Kalwar, M.A., Hussain, M., and Asghar, H., 2020. Petrography of Upper Nari Formation, Gandri Jabal, Pakistan. North American Academic Research, 3, 178–199.

Powell, C.M., 1979. A Speculative Tectonic History of Pakistan and Surroundings: Some constraints from Indian Ocean. In: Farah, A., De Jong, K.A. (Eds.), Geodynamics of Pakistan. Geological Survey of Pakistan, Quetta, 5–24.

Qamar, S., Shah, M.M., Janjuhah, H.T., Kontakiotis, G., Shahzad, A., and Besiou, E., 2023. Sedimentological, Diagenetic, and Sequence Stratigraphic Controls on the Shallow to Marginal Marine Carbonates of the Middle Jurassic Samana Suk Formation, North Pakistan. Journal of Marine Science and Engineering, 11, 1230.

Rashid, M., Luo, M., Ashraf, U., Hussain, W., Ali, N., Rahman, N., Hussain, S., Aleksandrovich Martyushev, D., Vo Thanh, H., and Anees, A., 2022. Reservoir quality prediction of gas-bearing carbonate sediments in the Qadirpur field: Insights from advanced machine learning approaches of SOM and cluster analysis. Minerals, 13, 29.

Raza, H.A., Ali, S.M., and Ahmed, R., 1990. Petroleum Geology of Kirthar sub-Basin and Part of Kutch Basin. Pakistan Journal of Hydrocarbon Research, 2, 29–73.

Reed, J.S., Eriksson, K.A., and Kowalewski, M., 2005. Climatic, Depositional and Burial controls on Diagenesis of Appalachian Carboniferous Sandstones: Qualitative and Quantitative methods. Sedimentary Geology, 176, 225–246.

Royden, L.H., and Clark, B.B., 2004. The Tibetan Plateau and Surrounding Regions. In: Pluijm, B.A.V.D., Marshak, S. (Eds.), Earth Structure. W.W. Norton & Company, New York, 525 – 534.

Rudmin, M., Banerjee, S., Sinkina, E., Ruban, A., Kalinina, N., and Smirnov, P., 2022. A study of iron carbonates and clay minerals for understanding the origin of marine ooidal ironstone deposits. Marine and Petroleum Geology, 142, 105777.

Saha, A., and Bhattacharya, B., 2022. Controls on near-surface and burial diagenesis of a syn-rift siliciclastic rock succession: A study from Permian Barren Measures Formation, Southern India. Sedimentary Geology, 436, 106170.

Salem, A.M., Ketzer, J.M., Morad, S., Rizk, R.R., and Al-Aasm, I.S., 2005. Diagenesis and Reservoir-Quality Evolution of Incised-Valley Sandstone: Evidence from the Abu Madi Gas Reservoirs (upper Miocene), the Nile Delta Basin, Egypt. Journal of Sedimentary Research, 75, 572–584. https://doi.org/10.2110/jsr.2005.047

Samtio, M.S., Hakro, A.A.A.D., Lashari, R.A., Mastoi, A.S., Rajper, R.H., and Agheem, M.H., 2021. Depositional Environment of Nari Formation from Lal Bagh Section of Sehwan Area, Sindh Pakistan. Sindh University Research Journal (Science Series), 53, 67–76.

Sarwar, G., and De Jong, K.A., 1979. Arcs, Oroclines, Syntaxes: the Curvatures of Mountain Belts in Pakistan. In: Farah, A., De Jong, K.A. (Eds.), Geodynamics of Pakistan. Geological Survey of Pakistan, Quetta, 341–349.

Schelling, D.D., 1999. Frontal structural geometries and detachment tectonics of the northeastern Karachi arc, southern Kirthar Range, Pakistan. Special Paper of the Geological Society of America, 328, 287–302. https://doi.org/10.1130/0-8137-2328-0.287

Schmidt, V., and McDonald, O.A., 1979. The role of secondary porosity in the course of sandstone diagenesis. In: Scholle, P.A., Schluger, P.R. (Eds.), Aspects of Diagenesis. Society of Economic Paleontologists and Mineralogists, Tulsa, USA, 175–207.

Selley, R.C., 1998. Elements of Petroleum Geology, 2nd ed. Academic Press: London.

Shah, S.M.I. (Ed.), 1977. Stratigraphy of Pakistan, Mem. 12. ed. Geological Survey of Pakistan, Quetta.

Shah, S.M.I. (Ed.), 2009. Stratigraphy of Pakistan, Mem. 22. ed. Geological Survey of Pakistan, Quetta.

Shar, A.M., Mahesar, A.A., Abbasi, G.R., Narejo, A.A., and Hakro, A.A.A.D., 2021a. Influence of diagenetic features on petrophysical properties of fine-grained rocks of Oligocene strata in the Lower Indus Basin, Pakistan. Open Geosciences, 13, 517–531. https://doi.org/10.1515/geo-2020-0250

Shar, A.M., Mahesar, A.A., Abbasi, G.R., Narejo, A.A., and Hakro, A.A.A.D., 2021b. Influence of diagenetic features on petrophysical properties of fine-grained rocks of Oligocene strata in the Lower Indus Basin, Pakistan. Open Geosciences, 13, 517–531. https://doi.org/10.1515/geo-2020-0250

Smewing, J.D., Warburton, J., Cernuschi, A., and Ul-Haq, N., 2002. Structural Inheritance in the Southern Kirthar Fold Belt. PAPG/SPE Annual Technical Conference, 22-23 November 2002, Islamabad, Pakistan.

Taylor, J.M., 1950. Pore-Space Reduction in Sandstones. Bulletin of American Assocaition of Petroleum Geologist 34, 701–716.

Ullah, S., Jan, I.U., Hanif, M., Latif, K., Mohibullah, M., Sabba, M., Anees, A., Ashraf, U., and Vo Thanh, H., 2022. Paleoenvironmental and bio-sequence stratigraphic analysis of the cretaceous pelagic carbonates of eastern tethys, sulaiman range, Pakistan. Minerals, 12, 946.

Umar, M., Friis, H., Khan, A.S., Kassi, A.M., and Kasi, A.K., 2011. The effects of diagenesis on the reservoir characters in sandstones of the Late Cretaceous Pab Formation, Kirthar Fold Belt, southern Pakistan. Journal of Asian Earth Sciences, 40, 622–635. https://doi.org/10.1016/j.jseaes.2010.10.014

Vredenburg, E.W., 1925. Description of Mollusca from the post-Eocene Tertiary formations of north-western India. Geological Survey of India, 50, 1–506.

Walker, T.R., 1974. Formation of Red Beds in Moist Tropical Climates: A Hypothesis. Bulletin of Geological Society of America, 85, 633–638. https://doi.org/10.1130/0016-7606(1974)85<633:FORBIM>2.0.CO;2

Wang, W., Lin, C., Zhang, X., Dong, C., Ren, L., and Lin, J., 2021. Provenance, clastic composition and their impact on diagenesis: A case study of the Oligocene sandstone in the Xihu sag, East China Sea Basin. Marine and Petroleum Geology, 126. https://doi.org/10.1016/j.marpetgeo.2020.104890

Worden, R.H., and Burley, S.D., 2003. Sandstone Diagenesis: The Evolution of Sand to Stone. In: Burley, Stuart D., Worden, Richard H. (Eds.), Sandstone Diagenesis: Recent and Ancient. International Association of Sedimentologists, 3–44. https://doi.org/10.1002/9781444304459.ch

Wu, D., Li, H., Jiang, L., Hu, S., Wang, Y., Zhang, Y., and Liu, Y., 2019. Diagenesis and reservoir quality in tight gas bearing sandstones of a tidally influenced fan delta deposit: The Oligocene Zhuhai Formation, western Pearl River Mouth Basin, South China Sea. Marine and Petroleum Geology, 107, 278–300. https://doi.org/10.1016/j.marpetgeo.2019.05.028

Zaid, S.M., and Al Gahtani, F., 2015. Provenance, diagenesis, tectonic setting, and geochemistry of Hawkesbury Sandstone (Middle Triassic), southern Sydney Basin, Australia. Turkish Journal of Earth Sciences, 24, 72–98. https://doi.org/10.3906/yer-1407-5

Zhang, H., Thanh, H.V., Rahimi, M., Al-Mudhafar, W.J., Tangparitkul, S., Zhang, T., Dai, Z., and Ashraf, U., 2023. Improving predictions of shale wettability using advanced machine learning techniques and nature-inspired methods: Implications for carbon capture utilization and storage. Science of The Total Environment, 877, 162944.

Zhang, K., Fang, X., Xie, Y., Guo, S., Liu, Z., and Wang, L., 2020. Diagenesis and Origination of Carbonate Cements in Deeply Buried Sandstones of the Eocene Es3 Member, Raoyang Sag, Bohai Bay Basin, China. Geofluids, 2020, 1–18.

Zhang, S., Wu, K., Liu, N., Peng, X., and Chen, Y., 2022. Microscopic Characteristics and Formation Mechanism of Effective Reservoirs in the Xihu Depression, China: The Important Role of the Poikilotopic Calcite Cements in Tide-Dominated Delta Systems. Minerals, 12, 1413.

Zhong, S., and Mucci, A., 1989. Calcite and aragonite precipitation from seawater solutions of various salinities: Precipitation rates and overgrowth compositions. Chemical Geology, 78, 283–299.

Zhu, H., Liu, G., Zhong, D., Zhang, T., Lang, J., and Yao, J., 2018. Diagenetic controls on reservoir quality of tight sandstone: A case study of the Upper Triassic Yanchang Formation Chang 7 sandstones, Ordos Basin, China. Earth Sciences Research Journal, 22, 129–138. https://doi.org/10.15446/esrj.v22n2.72251

Zou, C., Zhu, R., Liu, K., Su, L., Bai, B., Zhang, X., Yuan, X., and Wang, J., 2012. Tight Gas Sandstone Reservoirs in China: Characteristics and Recognition Criteria. Journal of Petroleum Science and Engineering, 88, 82–91.